ISSN 1063-7826, Semiconductors, 2015, Vol. 49, No. 4, pp. 547–550. © Pleiades Publishing, Ltd., 2015.
Original Russian Text © A.S. Saidov, Sh.N. Usmonov, M.S. Saidov, 2015, published in Fizika i Tekhnika Poluprovodnikov, 2015, Vol. 49, No. 4, pp. 557–560.

Liquid-Phase Epitaxy of the $(Si_2)_{1-x-y}(Ge_2)_x(GaAs)_y$ Substitutional Solid Solution ($0 \le x \le 0.91$, $0 \le y \le 0.94$) and Their Electrophysical Properties

A. S. Saidov^, Sh. N. Usmonov^^, and M. S. Saidov
Physicotechnical Institute, Academy of Sciences of Uzbekistan, Tashkent, 100084 Uzbekistan
e-mail: ^amin@uzsci.net, ^^sh_usmonov@rambler.ru
Submitted May 5, 2014; accepted for publication May 20, 2014

Abstract—$(Si_2)_{1-x-y}(Ge_2)_x(GaAs)_y$ substitutional solid solutions ($0 \le x \le 0.91$, $0 \le y \le 0.94$) are grown by liquid-phase epitaxy from a Pb-based solution–melt on Si substrates with the (111) crystallographic orientation. The chemical composition of the epitaxial films is studied by X-rays probe microanalysis, and the distribution profile of solid solution components is determined. Spectral dependences of the photosensitivity and photoluminescence of the n-Si–$p(Si_2)_{1-x-y}(Ge_2)_x(GaAs)_y$ heterostructures are studied at room and liquid-nitrogen temperatures. Two maxima are found in the photoluminescence spectra of the $(Si_2)_{1-x-y}(Ge_2)_x(GaAs)_y$ films ($0 \le x \le 0.91$, $0 \le y \le 0.94$) against the background of a broad emission spectrum. The fundamental maximum with an energy of 1.45 eV is caused by the band-to-band recombination of solid solution carriers, and an additional maximum with an energy of 1.33 eV is caused by the recombination of carriers with the participation of impurity levels of the Si–Si bond (Si_2 is covalently coupled with the tetrahedral lattice of the solid solution host).

DOI: 10.1134/S106378261504020X

1. INTRODUCTION

The modern development of microelectronics, nanoelectronics, and optoelectronics is creating interest in the synthesis and study of new semiconductor materials with various electrical properties. Studies of the technology of the fabrication and investigation of the electrical properties of binary and multicomponent complex semiconductor materials based on Group IV elements and III–V and II–VI semiconductor compounds showed the prospects of these materials. These studies indicate that it is possible to control their operational parameters and functional possibilities upon specific selection of components and doping impurities [1–8]. They can be used as active elements for the development of various optoelectronic devices as light-emitting diodes, photodiodes, detectors of optical and nuclear radiation, and photoconverters [9–13].

2. GROWTH PROCEDURE OF THE $(Si_2)_{1-x-y}(Ge_2)_x(GaAs)_y$ SOLID SOLUTION

The $(Si_2)_{1-x-y}(Ge_2)_x(GaAs)_y$ solid solutions were grown by liquid-phase epitaxy from a limited volume of Pb-based solution-melt in hydrogen. The substrates were Si wafers ~400 μm thick with the (111) crystallographic orientation of n-type conductivity 20 mm in diameter and a resistivity of ~0.5 Ω cm. Since the difference in the lattice constants of Si (5.41 Å) and GaAs (5.65 Å) is ~4.4%, the growth of GaAs on Si substrates without a buffer or $(Si_2)_{1-x}(GaAs)_x$ graded-gap layer ($0 \le x \le 1$) with a smoothly varying composition is very complex. Therefore, to smooth the crystal-lattice parameters and form a gradual transition from the Si substrate to the GaAs epitaxial layer, we used a buffer layer consisting of the components Si_2, SiGe, Ge_2, and GaAs. These components are isovalent to each other and the difference in the sums of the covalent radii of molecules Si_2 (2.34 Å), SiGe (2.39 Å), Ge_2 (2.44 Å), and GaAs (2.44 Å) is no larger that 4.3%. The sums of the covalent radii of the molecules Si_2 and SiGe, SiGe and Ge_2, SiGe and GaAs, and Ge_2 and GaAs differ within the limits of 2.1%. The mutual substitution of these molecules does not lead to strong deformation of the crystal lattice.

The composition of the Pb–Si–Ge–GaAs solution-melt was calculated based on reference data [14] and the results of preliminary experiments allowing for the solubility of the binary component. Silicon, Ge, and GaAs in liquid Pb are arranged at selected temperatures in the form of Si_2, Ge_2, and GaAs molecules, which is important for growing the substitutional solid solution.

The temperature of crystallization onset and the content of the solution-melt components were selected from the condition that the solution-melt should be saturated by all solid solution components

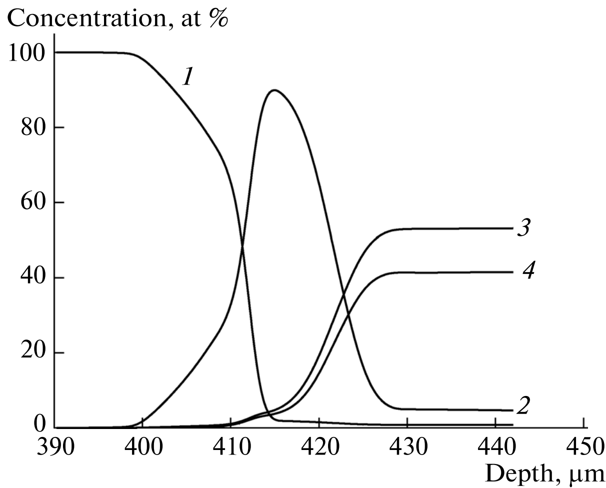

Fig. 1. Distribution profiles of (*1*) Si, (*2*) Ge, (*3*) Ga, and (*4*) As in the epitaxial layer of the $(Si_2)_{1-x-y}(Ge_2)_x(GaAs)_y$ solid solution ($0 \le x \le 0.91$, $0 \le y \le 0.94$).

and supersaturated with respect to Si. In this case, an epitaxial Si layer started to grow on the Si substrate. The solution-melt will be further supersaturated by both Ge and GaAs upon cooling. The quality of the grown films depends on the parameters of the production process: the crystallization temperature, distance between the substrates, and forced cooling rate of the solution-melt.

Epitaxial films of the $(Si_2)_{1-x-y}(Ge_2)_x(GaAs)_y$ solid solution with mirror surfaces were grown at the following production-process conditions: temperature of crystallization onset of 850°C, cooling rate of the solution-melt of 1 K/min, and gap between the substrates of 1–1.5 mm. The grown layers were of *p*-type conductivity.

3. STRUCTURAL AND PHOTOELECTRIC MEASUREMENTS OF THE PARAMETERS OF THE *n*-Si–*p*-$(Si_2)_{1-x-y}(Ge_2)_x(GaAs)_y$ HETEROSTRUCTURES ($0 \le x \le 0.91$, $0 \le y \le 0.94$)

3.1. X-Ray Structural Study of the Epitaxial Layer of the $(Si_2)_{1-x-y}(Ge_2)_x(GaAs)_y$ Solid Solution ($0 \le x \le 0.91$, $0 \le x \le 0.94$)

Studies of the chemical composition of the surface and a cleavage of the grown epitaxial layers were performed using a Jeol JSM 5910 LV-Japan X-ray microanalyzer. Analysis of the scan images showed the formation of a continuous epitaxial layer with tight adhesion to the substrate and transition sublayer of the variable-composition solid solution, in which Si, Ge, Ga, and As atoms are present.

Based on the results of electron-probe microanalysis, we determined the distribution profile of Si, Ge, Ga, and As atoms in the epitaxial layer of the $(Si_2)_{1-x-y}(Ge_2)_x(GaAs)_y$ solid solution (Fig. 1). The analysis of these results shows that the initial crystallization stage of the epitaxial layer is accompanied by the formation of a graded-gap sublayer of the $Si_{1-x}Ge_x$ substitutional solid solution with a gradual increase in the Ge content. The GaAs content in the beginning of the $Si_{1-x}Ge_x$ epitaxial sublayer ($0 \le x \le 0.20$) is <1 mol %, which is apparently caused by the energy minimization of elastic distortions of the solid solution crystal lattice associated with the difference in the sum of the covalent radii of atoms in the molecules of these components. Pairs of Si atoms Si_2 are further substituted with growth of the epitaxial film both by Ge_2 and GaAs molecules with a gradual increase in their concentration. Growth of the crystal lattice is accompanied by the more intense entering of Ge atoms into the film composition. This process occurs until a Ge content in the film of ~91 at %, which corresponds to the formation of a sublayer of the $(Si_2)_{1-x-y}(Ge_2)_x(GaAs)_y$ solid solution with a high Ge content ($0.20 \le x \le 0.91$, $0 \le y \le 0.08$). Further film growth kinetics is accompanied by the intense substitution of Ge sites of the crystal lattice by GaAs molecules, while the Si content in this sublayer is no higher than 1 at %. The molar content of GaAs in the layer rises with growth of the epitaxial layer reaching ~94 mol % on the film surface, while the Ge content lowers. Due to this, a sublayer of $(Ge_2)_{1-x}(GaAs)_x$ is formed ($0.09 \le x \le 0.94$). The solid solution surface layer to a large degree will be largely characterized by crystal-lattice parameters inherent to GaAs. Thus, with the corresponding thermodynamic conditions of the production process, we can attain a gradual transition from the Si sublayer to GaAs using a transition layer consisting of the $(Si_2)_{1-x-y}(Ge_2)_x(GaAs)_y$ substitutional solid solution ($0 \le x \le 0.91$, $0 \le y \le 0.94$).

3.2. Photoluminescence of an Epitaxial Layer of the $(Si_2)_{1-x-y}(Ge_2)_x(GaAs)_y$ Solid Solution ($0 \le x \le 0.91$, $0 \le x \le 0.94$)

The photoluminescence (PL) spectrum of an epitaxial layer of the $(Si_2)_{1-x-y}(Ge_2)_x(GaAs)_y$ solid solution ($0 \le x \le 0.91$, $0 \le y \le 0.94$) ~25 μm thick is shown in Fig. 2. The PL was excited by red laser radiation in the intrinsic absorption region of a wide-gap alloy component, i.e., GaAs, on the epitaxial-layer side at liquid-nitrogen temperature (77 K). It is seen from Fig. 2 that the PL spectrum has a broad band, which envelopes the near infrared region of the emission spectrum from 0.81 to 1.08 μm peaked at a wavelength of $\lambda = 0.855$ μm, which corresponds to a photon energy of $E_{ph} = 1.45$ eV. This peak is caused by the band-to-band recombination of free carriers in the surface epitaxial layer ~3 μm thick of the $(GaAs)_{0.90}(Ge_2)_{0.09}(Si_2)_{0.01}$ substitutional solid solution

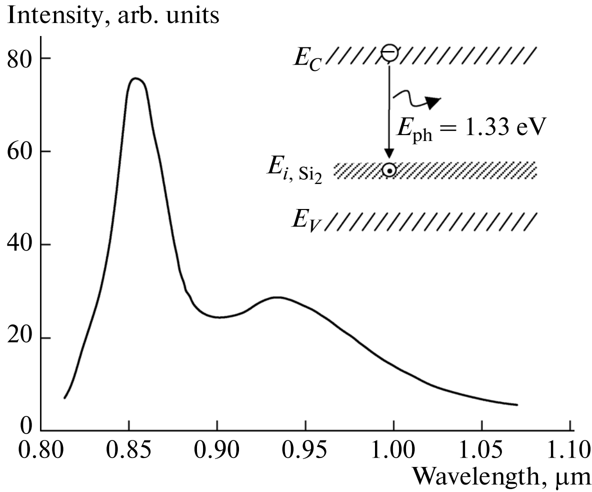

Fig. 2. Photoluminescence spectrum of the $(Si_2)_{1-x-y}(Ge_2)_x(GaAs)_y$ solid solution ($0 \le x \le 0.91$, $0 \le y \le 0.94$) at 77 K. The inset shows the energy-band diagram of the $(GaAs)_{0.90}(Ge_2)_{0.09}(Si_2)_{0.01}$ solid solution with a spread band of energy levels $E_{i,\,Si_2}$ (E_C is the conduction band and E_V is the valence band).

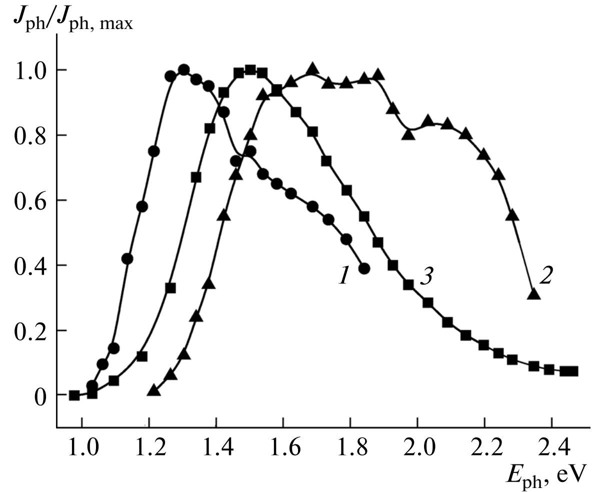

Fig. 3. Dependences of the photocurrent ratio to its maximal value for the n-Si–p-$(Si_2)_{1-x-y}(Ge_2)_x(GaAs)_y$ heterostructure ($0 \le x \le 0.91$, $0 \le y \le 0.94$) at (*1*) 300 and (*2*) 77 K as well as (*3*) the p-Si–n-Si reference structure at 300 K on the photon energy.

(Fig. 1), the band gap E_g of which is narrower than E_g(GaAs) = 1.51 eV and wider than E_g(Si) = 1.16 eV and E_g(Ge) = 0.73 eV at 77 K. A comparatively weak but a rather wide emission peak is distinguished in the PL spectrum in a long-wavelength region at λ = 0.933 μm, which corresponds to a photon energy of E_{ph} = 1.33 eV. The presence of such peak against the background of broad emission spectrum apparently points to the emergence of the spread band of energy levels of the Si–Si covalent bond ($E_{i,\,Si_2}$) located in the band gap of the $(GaAs)_{0.90}(Ge_2)_{0.09}(Si_2)_{0.01}$ substitutional solid solution (Fig. 2, inset). Since the incident laser radiation is absorbed in the surface region of the film ~3 μm thick, the luminescent radiation originates in the film sublayer, where the broad-band GaAs is a base component. This is additionally evidenced by a broad emission band with a higher intensity peaked at λ = 0.855 μm. The Si content in the surface region of the film is ~1 at %; consequently, the spread band of energy levels at E_{ph} = 1.33 eV is possibly caused by the radiative recombination of carriers with participation of the Si–Si bond, which is located in the environment of the GaAs-enriched sublayer of the tetrahedral lattice of the $(Si_2)_{1-x-y}(Ge_2)_x(GaAs)_y$ solid solution. It is known that the ionization energy of the Si–Si covalent bond, which is arranged in the tetrahedral lattice of pure Si at 77 K, is 1.16 eV. However, when the Si–Si bond is located in the environment of comparatively strongly coupled Ga–As atoms, the energy of the Si–Si bond increases to 1.33 eV at 77 K due to hybridization of the electron shells of the atoms of Si_2 and GaAs molecules and determines the emergence of the spread band of energy levels of the Si–Si covalent bond in the band gap of the $(GaAs)_{0.90}(Ge_2)_{0.09}(Si_2)_{0.01}$ solid solution. Since the Si–Si covalent bond is saturated, it can be only of the donor type.

3.3. Spectral Dependence of the Photosensitivity of the n-Si–p-$(Si_2)_{1-x-y}(Ge_2)_x(GaAs)_y$ Heterostructures ($0 \le x \le 0.91$, $0 \le y \le 0.94$)

To study the spectral dependence of the solid solution photosensitivity, n-Si–p-$(Si_2)_{1-x-y}(Ge_2)_x(GaAs)_y$ heterostructures ($0 \le x \le 0.91$, $0 \le x \le 0.94$) with an epitaxial layer ~25 μm thick were fabricated. For comparison, we also studied p-Si–n-Si structures with an n-Si diffusion layer ~1 μm thick. Figure 3 shows the dependence of the photocurrent ratio to its maximal value ($J_{ph}/J_{ph,\,max}$) for the studied heterostructures at 300 and 77 K on the photon energy (E_{ph}) when illuminating the face surfaces of the samples. It is seen from Fig. 3 that the spectral photosensitivity region of the n-Si–p-$(Si_2)_{1-x-y}(Ge_2)_x(GaAs)_y$ heterostructure (curve *1*) is shifted to the long-wavelength region compared with the p-Si–n-Si structure (curve *3*). A shift of the sensitivity maximum by 0.2 eV is also observed. This evidences the active participation of the Ge-enriched alloy sublayer in photogeneration (Fig. 1); its band gap is narrower than E_g of Si. The decay of the heterostructure photosensitivity in the short-wavelength region is apparently caused by the burial depth (l_{p-n}) of the separating field of the p–n junction, which is determined by the thickness of the epitaxial layer in our case: $l_{p-n} \approx$ 25 μm.

It is seen from Fig. 3 (curve *2*) that $J_{ph}/J_{ph, max}$ of the n-Si–p-$(Si_2)_{1-x-y}(Ge_2)_x(GaAs)_y$ heterostructure at 77 K starts to abruptly increase beginning at a photon energy of 1.21 eV and reaches its maximum at E_{ph} = 1.69 eV. After this, it decreases nonmonotonically, and bending and maxima at 1.88 and 2.06 eV are observed. They are apparently caused by the difference in the composition of the $(Si_2)_{1-x-y}(Ge_2)_x(GaAs)_y$ solid solution ($0 \le x \le 0.91$, $0 \le y \le 0.94$) over the epitaxial-layer depth (Fig. 1). The maximum at 1.69 eV is apparently largely determined by the influence of Ge, the increase in the region 1.77–1.88 eV is caused by Si, and the increase in region $E_{ph} \gtrsim 2$ eV is caused by a wide-gap alloy component, i.e., GaAs. It should be noted that the interaction of the molecules of the solid solution components affects the arrangement of these maxima. The ionization energies of Ge–Ge, Si–Si, and Ga–As covalent bonds in the $(Si_2)_{1-x-y}(Ge_2)_x(GaAs)_y$ solid solution due to the interaction of these molecules differ from the energy in the situation when they are in the corresponding pure semiconductor material.

4. CONCLUSIONS

Thus, we showed the fundamental possibility of growing epitaxial films of the $(Si_2)_{1-x-y}(Ge_2)_x(GaAs)_y$ solid solution ($0 \le x \le 0.91$, $0 \le y \le 0.94$) with a high GaAs content (as high as 94 mol %) on a film surface through a buffer layer consisting of the $(Si_2)_{1-x}(Ge_2)_x$ solid solution ($0 \le x \le 0.91$) on Si substrates with the (111) crystallographic orientation by liquid-phase epitaxy from a Pb-containing solution-melt.

The Si–Si covalent bonds in the $(GaAs)_{0.90}(Ge_2)_{0.09}(Si_2)_{0.01}$ solid solution with a band gap of 1.45 eV at 77 K form a deep spread band of donor energy levels arranged 1.33 eV below the conduction-band bottom of the solid solution. The grown epitaxial layers can be used as a substrate material for the further growth of III–V semiconductor compounds or their solid solutions having crystal-lattice parameters close to the GaAs lattice parameter. They can also be used as a photoactive semiconductor material for designing optoelectronic devices operating in the near-infrared emission spectral region.

ACKNOWLEDGMENTS

We thank A.Yu. Leiderman for valuable advice and discussion.

REFERENCES

1. R. Ragan, K. S. Min, and H. A. Atwater, Mater. Sci. Eng. B **87**, 204 (2001).
2. M. F. Fyhn, J. Lundsgaard Hansen, J. Chevallier, and A. NylandstedLarsen, Appl. Phys. A **68**, 259 (1999).
3. A. S. Saidov, Sh. N. Usmonov, M. U. Kalanov, A. N. Kurmantaev, and A. N. Bakhtybaev, Phys. Solid State **55**, 45 (2013).
4. A. S. Saidov, Sh. N. Usmonov, and U. P. Asatova, Semiconductors **46**, 1088 (2012).
5. A. S. Saidov, M. S. Saidov, Sh. N. Usmonov, A. Yu. Leiderman, M. U. Kalanov, K. G. Gaimnazarov, and A. N. Kurmantaev, Phys. Solid State **53**, 2012 (2011).
6. A. S. Saidov, M. S. Saidov, Sh. N. Usmonov, and U. P. Asatova, Semiconductors **44**, 938 (2010).
7. Sh. N. Usmonov, A. S. Saidov, A. Yu. Leiderman, D. Saparov, and K. T. Kholikov, Semiconductors **43**, 1092 (2009).
8. A. S. Saidov, Sh. N. Usmonov, K. T. Kholikov, and D. Saparov, Tech. Phys. Lett. **33**, 701 (2007).
9. A. N. Baranov, B. E. Dzhurtanov, A. N. Imenkov, A. A. Rogachev, Yu. M. Shernyakov, and Yu. P. Yakovlev, Sov. Phys. Semicond. **20**, 1385 (1986).
10. G. Bougnot and F. de Lannoy, J. Electrochem. Soc. **135**, 783 (1988).
11. S. P. Kozyrev, Semiconductors **43**, 911 (2009).
12. K. Chilukuri, M. J. Mori, C. L. Dohrman, and E. A. Fitzgerald, Semicond. Sci. Technol. **22**, 29 (2007).
13. R. Ginige, B. Corbett, M. Modreanu, C. Barrett, J. Hilgarth, G. Isella, D. Chrastina, and H. von Koenel, Semicond. Sci. Technol. **21**, 775 (2006).
14. M. Hansen and K. Anderko, *Constitution of Binary Alloys* (McGraw-Hill, Toronto, London, New York, 1958), Vol. 2.

Translated by N. Korovin